POLITECNICO DI TORINO
Repository ISTITUZIONALE

Shield for Sand: An Innovative Barrier for Windblown Sand Mitigation

Original
Shield for Sand: An Innovative Barrier for Windblown Sand Mitigation / Bruno, L., Coste, N., Fransos, D., Lo Giudice, A., Preziosi, L., Raffaele, L.. - In: RECENT PATENTS ON ENGINEERING. - ISSN 1872-2121. - ELETTRONICO. - 12:3(2018), pp. 237-246. [10.2174/1872212112666180309151818]

Availability:
This version is available at: 11583/2709729 since: 2018-11-15T15:57:11Z

Publisher:
Bentham Science

Published
DOI:10.2174/1872212112666180309151818

Terms of use:

This article is made available under terms and conditions as specified in the corresponding bibliographic description in the repository

Publisher copyright

(Article begins on next page)

27 November 2026

Recent Patents on Engineering, 2018, *12*, 237-246

RESEARCH ARTICLE

Shield for Sand: An Innovative Barrier for Windblown Sand Mitigation

Luca Bruno[1,4,*], Nicolas Coste[3,4], Davide Fransos[3,4], Andrea Lo Giudice[2,3,4], Luigi Preziosi[2,4] and Lorenzo Raffaele[1,4]

[1]*Department of Architecture and Design, Politecnico di Torino, Torino, Italy;* [2]*Department of Mathematical Sciences "Giuseppe Luigi Lagrange", Politecnico di Torino, Torino, Italy;* [3]*Optiflow Company, Marseille, France and* [4]*Windblown Sand Modeling and Mitigation joint research group, Italy*

Abstract: ***Background***: Windblown sand mitigation for civil structures in arid environment is crucial. Indeed, the number of railways crossing deserts and arid lands is increasing. A number of sand mitigation measures already exist. Among them, sand barriers are particularly intended for line-like infrastructures. We reviewed patented sand barriers on the basis of their shape and porosity.

Objective: A new solid barrier for windblown sand mitigation called Shield for Sand is presented. Shield for Sand has been designed with the aim of maximizing the sand trapping efficiency through an upper windward deflector and simplifying its maintenance by complaining to sand removal machines. The development of Shield for Sand follows the path traced by the Technology Readiness Level scale.

Methods: The preliminary design of Shield for Sand has been supported by computational simulations of the wind flow around the barrier. Then, Shield for Sand has been tested in a wind tunnel with drifting sand in order to assess its efficiency. Both computational and experimental approaches allow an increase of the Technology Readiness Level.

Results: The reversed flow induced by Shield for Sand increases its sand accumulation potential with respect to similar existing sand mitigation measures, such as the straight vertical wall. The efficiency of Shield for Sand resulting from the wind tunnel test is very high and almost constant with increasing sand accumulation level.

Conclusion: The Shield for Sand working principles and performances are confirmed excellent. Final full-scale in-situ experiments are necessary to test the barrier under real environmental operational conditions.

ARTICLE HISTORY

Received: October 24, 2017
Revised: January 30, 2018
Accepted: March 01, 2018

DOI:
10.2174/1872212112666180309151818

Keywords: Windblown sand, mitigation measures, barrier, railway infrastructure, technology readiness levels, shield for sand.

1. INTRODUCTION

The attempt to mitigate windblown sand arises from the interaction with a number of human activities and civil structures and infrastructures in the desert and arid environments. In particular, windblown sand affects roads [1], railways [2], industrial facilities and pipelines [3], farms [4], towns, and buildings [5]. Windblown sand transport results from soil erosion and causes sand accumulation around human-built obstacles. Line-like infrastructures, such as railways, are the most sensitive to such an issue.

In the last 10 years, the number of railways crossing deserts or arid zones has increased. Railways crossing regions affected by windblown sand are particularly located in the desert belt at the northen horse latitudes. Fig. (**1**) depicts a number of existing, under construction, and planned railway tracks ranging from China to North Africa. In particular, North-western China comprehends a total length of 10.000 Km of affected railways, *e.g.* the Lanzhou−Xinjiang line across the Gobi desert, the Xining-Lhasa line along the Tibet plateau, the Linhai-Ceke line across the Ulanbuhe, Yamaleike, and the Badain Jaran Deserts. Apart from China, the majority of the in-service desert railways are located in the Middle East – North Africa (MENA) region, *e.g.* the Iranian railway Network comprehending an overall length of about 400 km of track exposed to windblown sand, the 550 Km long Dammam–Riyadh line in Kingdom of Saudi Arabia (KSA), the 2.400 Km long North South Railway in KSA, the 266 Km long phase 1 of the Etihad Rail network in United Arab Emirates (UAE). The railway lines crossing deserts and arid regions are expected to rapidly grow in the next years. In particular, the 30.000 Km long Arab Network Railway will connect all the Arab League Countries [6]; the 2.217

*Address correspondence to this author at the Department of Architecture and Design, Politecnico di Torino, P.O. Box: I-10125, Torino, Italy;
Tel: +39-011-090-4870; E-mail: luca.bruno@polito.it

 © 2018 Bentham Science Publishers

Recent Patents on Engineering

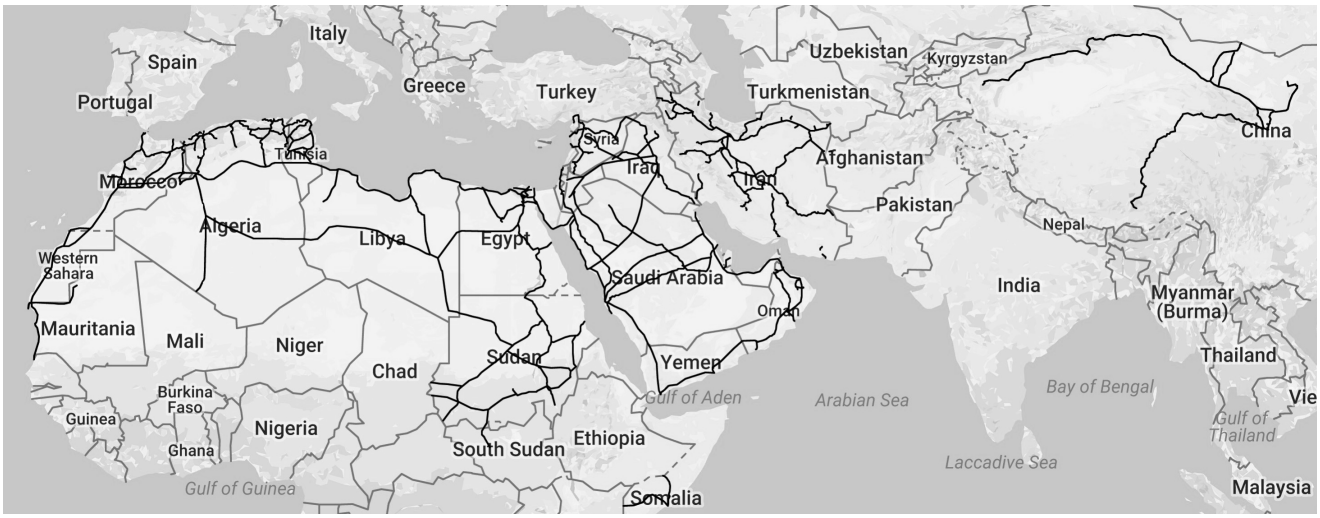

Fig. (1). Railways affected by windblown sand along the desert belt in the Northern Hemisphere.

Km long Gulf Railway will link the states member of the Arab Gulf Co-operation Council [6]; a 1373 km long railway line, segment of the Eurasian Land Bridge, will connect China to Iran passing through Kyrgyzstan, Tajikistan and Afghanistan [7].

The effects of windblown sand on railways are manifold and involve several aspects of the infrastructure. A number of these effects have occurred in the recent past along with the built railway's lines crossing arid regions, *e.g.* the Qinghai-Tibet Railway [2], the North-South Mineral Line [8] and the Lanzhou−Xinjiang line [9]. Sand deposition on the infrastructure can lead to the contamination of ballast, which leads in turn to the increasing of train-induced vibrations and consequently damage of sleepers, rail pads and rails [10]. It causes the jamming of turnouts, the covering of the signalling systems, the grinding of rails, the wearing of wheels [11] and train elements in general. This results in increased costs due to the repeated maintenance and loss of capacity of the line [12], *i.e.* reduced train speed and delays. Furthermore, windblown sand can lead to disastrous events causing even danger for users, such as train derailment and window breaking [9].

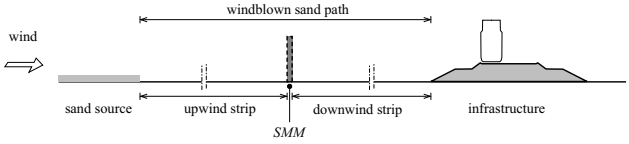

Fig. (2). Sand mitigation measure (SMM).

With the increasing railway tracks in desert areas, effective design solutions to cope with windblown sand issues are mandatory. A number of windblown Sand Mitigation Measures (SMM) have been proposed so far. Generally, they aim at avoiding sand deposition on the protected infrastructure. This can be achieved following different working principles, such as promoting sand deposition away from the protected infrastructure by decreasing the wind speed, reducing wind erosion over the sand sources, or, alternatively, increasing wind erosion over the infrastructure. The sand mitigation measures that promote sand deposition away from the infrastructure translate into line-like devices located between the sand source and the infrastructure (Fig. **2**). These mitigation measures range from stabilized sand berms and ditches to windblown sand barriers. In the following, we will focus on windblown sand barriers since they are usually preferred to berms and ditches. Indeed, the construction and maintenance costs of both stabilized sand berms and ditches are higher than the ones related to windblown sand barriers.

In the scientific literature, different kinds of SMMs have been studied and reviewed. Fences are conceived as nets or sheets with smeared porosity [13]. They reduce the wind velocity around them and induce in turn sand accumulation on both upwind and downwind strips (see Fig. **(2)**). Fence porosity ratio is commonly considered as the most important parameter driving their performance. Porous barriers are conceived as solid barriers with localized porosity, *i.e.* openings of the same order of magnitude of the barrier height. They act analogously to smeared porosity fences and additionally generate large turbulent eddies in their wake. Some examples in the literature are represented by the hanging windshield wall and bottom-opening windshield wall examined in Cheng *et al*. [14], and the hanging type concrete wall described in Cheng and Xue [15]. Solid barriers do not present any porosity. They are scarcely investigated in the scientific literature [16]. They induce an upwind vortex in the mean wind flow, and sand sedimentation mainly occurs on the upwind strip [17]. Their trapping performances are expected to decrease with increasing levels of accumulated sand. Compared to porous fences, vertical solid barriers of equal height trap a lower volume of sand per unit length. Indeed, porous barriers allow sand sedimentation on both upwind and downwind strips. However, solid barriers should be preferred as SMM around infrastructures since they prevent the sand accumulation in the infrastructure corridor and lead to a cheaper sand removal.

In the engineering practice, both porous and solid barriers are employed as SMM along railways. Net fences are adopted along the Etihad railway (UAE) and have been tested along the North-South line (KSA). They are also largely employed in oil industry [18]. Straight Vertical Wall (SVW) has

been tentatively tested. For example, a 4-meter high SVW was proposed as SMM in the preliminary design of the Segment 1 of the Oman National Railway Network [19]. A 1.5-meter high SVW was recently tested in situ along the Mecca-Medina high-speed railway line in KSA [20], showing questionable performances. Solid barriers other than SVW remain scarcely exploited.

1.1. SMM Patent Landscaping

In the following, patented SMMs are reviewed, with particular attention to barriers, and on the basis of their categorization.

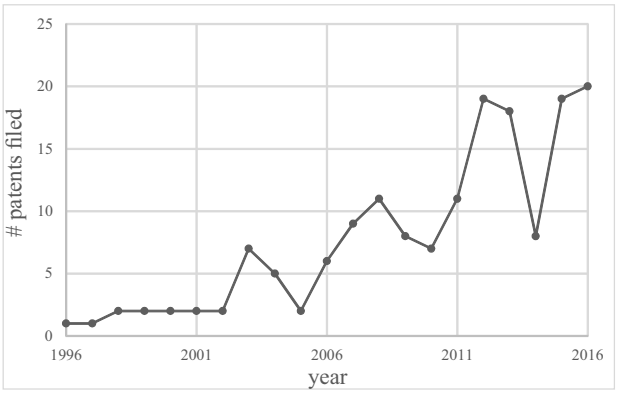

Fig. (3). Trend of the inventive activity from 1996 to 2016.

The patent landscaping has been performed thorough Orbit© patent database. The considered technologies are classified by the International Patent Classification (IPC) codes E01F 7/02 “Snow fences or similar devices, *e.g.* devices affording protection against sand drifts or side-wind effects” and E04H 17/00 "Fencing, *e.g.* fences, enclosures, corrals”. Fig. **(3)** shows the trend of the inventive activity along time, *i.e.* the number of filed patents in the last 20 years. Between 1996 and 2016, 162 SMM patents were filed. The overall increasing trend testifies the growing industrial interest on the topic. In particular, 52% of patents have been filed during the last five years. This suggests an increasing patenting potential in the next coming years.

The windblown sand barrier is about 60% of all patented SMMs. In the following, we propose a new categorization of sand barriers, in order to map this wide patent landscape. Some categories (Smeared-porosity fences, barriers with localized porosity, solid barriers) are taken from the existing scientific literature. Other categories (free end deflectors, deflecting vanes) are introduced on the basis of the patent landscaping itself. Fig. **(4)** shows the distribution of patents concerning windblown sand barriers and one patent example for each category. Fences and localized-porosity barrier account for more than 60% of the total, whilst solid barriers and deflectors account for about 15% each. Finally, 8% of the total amount is represented by a combination of the above devices.

Smeared-porosity fences, *e.g.* [21-23], are usually addressed to prevent erosion from sand dunes or stockpiles and to promote sand dune stabilization or dune growing in industrial, coastal or environmental engineering applications. Indeed, they are recommended in dune-building applications when the fast formation of the dune is required and sand removal is not necessary. *Localized-porosity barriers* [24, 25] have been patented and adopted also in railway engineering applications. Basic vertical s*olid barriers, e.g.* [26] are usually intended to act as both windbreakers and SMM. Novelty and inventive step of such barriers rely on the adopted materials or construction processes rather than in the well-known working principle. Some aerodynamically shaped solid barriers with different geometries have been patented [27, 28]. However, the inventors have only qualitatively conjectured their aerodynamic and trapping performances. *Deflectors* are conceived to take advantage from the wind acceleration induced by them to promote windblown sand transport or alternatively sedimented sand erosion. They can be subdivided into *free end* deflectors [29-31] and deflecting *vanes* [32] respectively. In particular, free end deflectors accelerate the wind upward and are conjectured to make the flying sand cross over the infrastructure. They have been proposed for road and railway applications, and for windblown snow or sand. The conjectured working principle looks physically sound for snow, while it seems questionable for sand because of its density. Deflecting vanes locally accelerate downwards the wind in their wake, close to the downwind road pavement. They are conjectured to keep it free of sand.

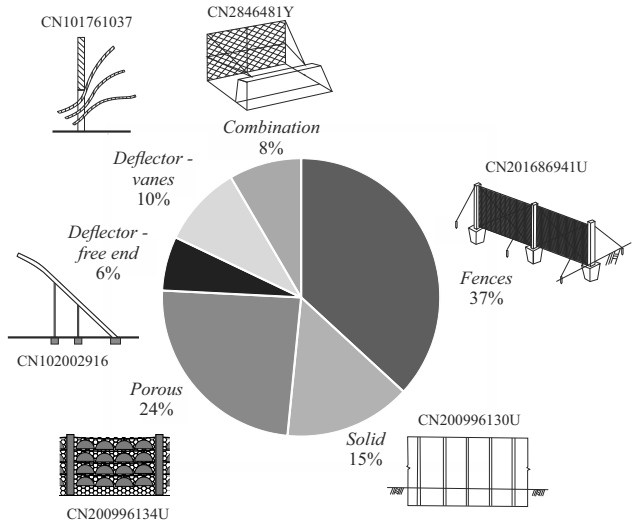

Fig. (4). Windblown sand barriers classification and distribution.

This study aims at presenting and demonstrating an innovative patented aerodynamically shaped solid barrier called Shield for Sand, owned by Politecnico di Torino. Shield for Sand innovative working principles, its components and its development plan are presented in Section 2. In Section 3, the methods adopted in order to demonstrate Shield for Sand working principles and assess its performance are reported. Results and discussion are provided in Section 4. Finally, conclusion and perspectives are outlined in Section 5.

2. SHIELD FOR SAND: WORKING PRINCIPLES AND TECHNOLOGY DEVELOPMENT

Very recently, Bruno *et al*. [33] have proposed a novel concept of solid barrier called Shield for Sand (S4S), patented by Politecnico di Torino (Fig. **(5)**). S4S cross-section ge-

ometry is generally characterized by three parts: 1. a foundation; 2. a lower quasi-vertical part; and 3. an upper windward concave deflector (Fig. **5a**). The values of the cross section main geometrical parameters depend on the specific construction site, *i.e.* the magnitude of the incoming sand flux.

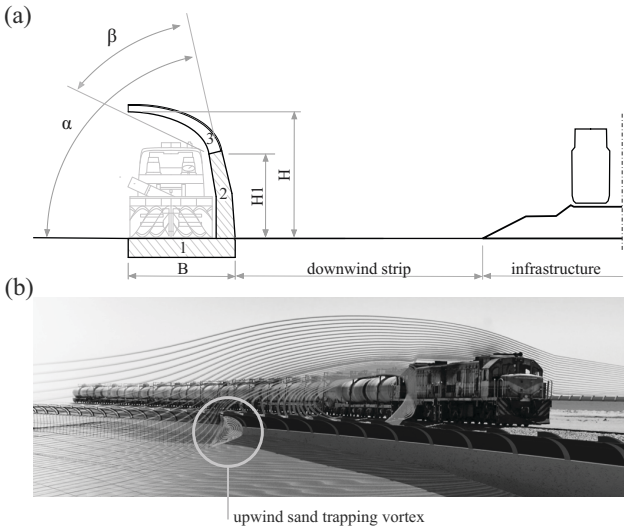

Fig. (5). S4S: geometry of the barrier (**a**) and rendering along a mitigated railway with simulated streamlines (**b**).

The three parts and their shape ensure functional requirements and the barrier working principles. The foundation opposes the overturning moment induced by both wind-induced load and passive trapped sand pressure. The quasi-vertical part allows an easy clearance of the accumulated sand by means of removal machines: For the sake of clarity, Fig. (**5a**) includes the front view of an actual sand blower machine [34]. The upper windward concave deflector is the key component in ensuring S4S innovative working principles: it promotes local downward deflection of the wind flow upwind the barrier, and in turn, maximizes the size of the induced upwind recirculation vortex (Fig. **5b**). The local reversed flow strongly decreases the velocity gradient close to the ground, and consequently the wall shear stress $\tau = \mu\, \partial u/\partial z|_{z=0}$. Sedimentation is guarantee where τ is lower than a threshold value τ_t which depends on the physical properties of the sand at the construction site [35]. As a result, the upwind vortex induced by S4S acts as a sand trapping one. Qualitatively, the larger the upwind vortex is, the higher the sand trapping performances, that is: i. sand is accumulated along the upwind strip only, ii. the volume of the trapped sand is as large as possible; iii. the trapping vortex still holds also for high levels of accumulated sand, and high trapping efficiency in turn.

Alternative construction methods, embodiments and materials can be specified for each part of S4S notwithstanding the general principles above. Options should comply with the construction requirements for civil engineering applications (simplicity of construction/prefabrication/assembling and maintenance, durability), and use building components possibly already employed in the industrial chain of other kinds of barriers (such as noise or wind barriers) in the Country where the barrier is built. For instance, the render in Fig. (**5b**) depicts a solid reinforced concrete continuous vertical wall, while the windward concave deflector is formed by pointwise curved steel pillars and a steel deflecting panel fixed at its intrados.

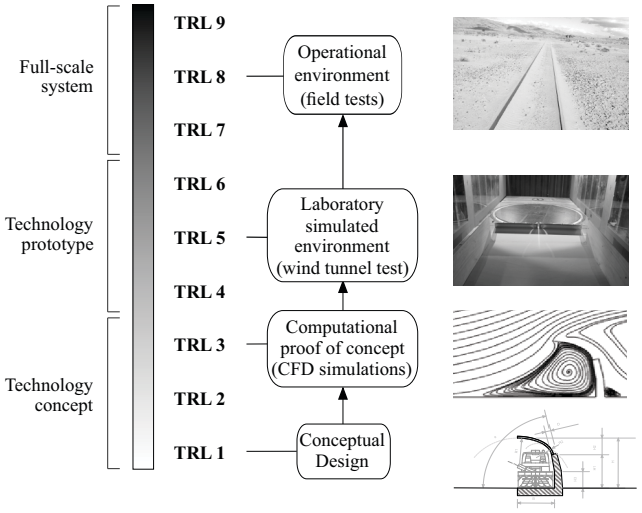

Fig. (6). S4S Technology Readiness Level.

The development of a patented technology shall reach an appropriate level of maturity to allow its actual application under operational environmental conditions. The so-called Technology Readiness Level (TRL) is a method of estimating, managing and developing a technology. Conceived by NASA in the Seventies [36], TRL is today widely adopted in a number of technological fields and by Research & Development institutions, *e.g.* the H2020 EU framework program. TRLs are based on a scale ranging from 1 to 9. For simplicity, TRL scale can be roughly subdivided into three parts, which refer to corresponding distinct stages of development of the selected technology.

In Fig. **(6)**, the general TRL scale is summarized and referred to the S4S development process. In the first part (TRL1-3), the S4S technology concept is investigated by means of basic research on windblown sand phenomena [37] and engineering constraints to be fulfilled. S4S barrier is patented [33]. The concept is proved by assessing its working principle and aerodynamic performances by means of Computational Fluid Dynamics (CFD) simulations [17]. This part corresponds to the conceptual and preliminary design phases in Civil Engineering. In the second part (TRL4-6), S4S prototype is tested in laboratory environment conditions in order to validate/demonstrate the technology. In particular, wind tunnel tests with windblown sand are performed on a scaled mockup and its trapping performances are measured [38]. This part corresponds to the detailed design phase in Civil Engineering. In the third part (TRL7-9), the full-scale system is tested under operational environmental conditions towards system qualification, production process launching and commercial deployment. This part corresponds to the as-built design phase in Civil Engineering [39].

The scientific approach to windblown sand mitigation is at its early-stage. As a result, Research & Development activities often follow trial and error procedures resulting in substantial additional costs. To the Author's best knowledge, there are no studies devoted to the development of SMMs in the framework of TRL. In the following, the applied meth-

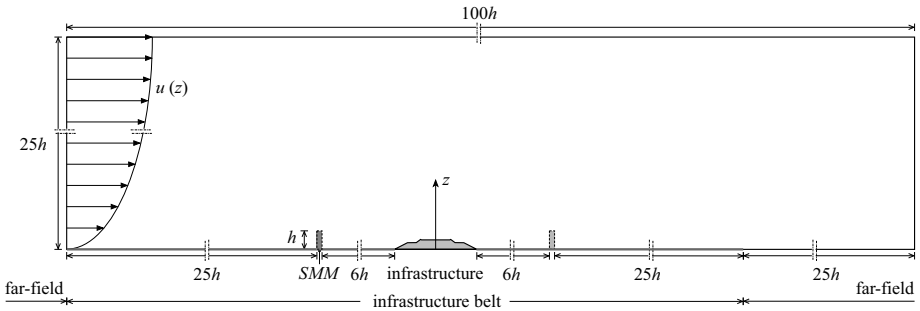

Fig. (7). Sketch of the computational domain.

ods and obtained results to conceive and validate S4S by increasing its TRL are provided and discussed.

3. METHODS

In the following, the methods adopted to develop and validate S4S are reported. The performances of S4S have been quantitatively assessed in two distinct phases. First, a computational simulation is used to demonstrate the conceptual working principles and obtain some preliminary metrics for the performance (TRL3). Secondly, a wind tunnel test is performed on a prototype of S4S to simulate the real environmental working conditions and assess its sand-trapping performance (TRL5).

3.1. Computational Simulation

A pure aerodynamic study has been performed in order to investigate the effect of S4S on the wind flow and to analyze the implications in terms of performance of the SMM as sedimentation-promoter. Since wall shear stress depends only on wind flow field, such a study allows shedding some light on the zones in which sand erosion and sand sedimentation take place due to the presence of the barrier. The mean aerodynamic behavior is obtained since the deposition process takes several months. Indeed, wind and sand sub-domains present two different characteristic timescales. A Computational Fluid Dynamic (CFD) simulation is carried out, using the Reynolds Averaged Navier-Stokes (RANS) approach. The Finite Volume open source code OpenFoam© is used to numerically evaluate the flow-field. The RANS momentum and mass conservation equations read:

$$\frac{\partial \bar{u}_i}{\partial x_i} = 0 \tag{1}$$

$$\bar{u}_j \frac{\partial \bar{u}_i}{\partial x_j} = -\frac{1}{\rho}\frac{\partial \bar{p}}{\partial x_i} + \frac{\partial}{\partial x_j}\left[\upsilon\left(\frac{\partial \bar{u}_i}{\partial x_j} + \frac{\partial \bar{u}_j}{\partial x_i}\right)\right] - \frac{\partial}{\partial x_j}(\overline{u'_i u'_j}) \tag{2}$$

Given the turbulent flow, SST $\kappa - \omega$ model, developed by Menter [39] and modified by Menter *et al*. [40], has been selected to close the equations:

$$\bar{u}_i \frac{\partial k}{\partial x_i} = \frac{\partial}{\partial x_i}\left[(\sigma_k \upsilon_t + \upsilon)\frac{\partial k}{\partial x_i}\right] + \tilde{P}_k - \beta^* k\omega \tag{3}$$

$$\bar{u}_i \frac{\partial \omega}{\partial x_i} = \frac{\partial}{\partial x_i}\left[(\sigma_\omega \upsilon_t + \upsilon)\frac{\partial \omega}{\partial x_i}\right] + \alpha\frac{\omega}{k}P_k - \beta\omega^2 + (1 - F_1)\frac{2\sigma_\omega}{\omega}\frac{\partial k}{\partial x_i}\frac{\partial \omega}{\partial x_i}. \tag{4}$$

where k is the turbulent kinetic energy, ω is the dissipation rate and υ_t is the turbulent kinematic viscosity. The definition of the other terms can be found in Menter *et al*. [40]. Taking advantage of symmetry, a 2D computational domain (sketched in Fig. **(7)**) has been adopted. The boundary conditions have been set in order to correctly reproduce arid-zone environment features. In particular, the incoming wind velocity profile is prescribed by the log-law $u(z) = u_*/k\log((z + z_0)/z_0)$, where u^* is the friction velocity, $\kappa = 0.41$ is the Von Karman constant, and $z_0 = 1e - 2[m]$ is the aerodynamic roughness of the incoming wind. The prescriptions of Richards and Norris [41] are followed to set the inlet profile of $k(z)$ and $\omega(z)$. No-slip conditions are imposed on the ground surface and at all the walls. A typical aeolian sand grains diameter $d = 0.25\ mm$ has been assumed, leading to a wall shear stress threshold $\tau_t = 0.1\ kg/(m\ s^2)$.

3.2. Wind Tunnel Testing

A 1:10 scale prototype of S4S is tested in the wind tunnel L1-B at the von Karman Institute for Fluid Dynamics (Belgium). The prototype consists of three parts: Two lateral non-transparent elements made of wood and aluminum, and a central transparent short section made in Plexiglas. Two lateral end-plates are placed next to the lateral free-ends in order to reduce the end-tip aerodynamic effects. A reference wind tunnel free stream velocity equal to $U = 9$m/s is set. The adopted sand has a mean grain diameter $d \approx 0.34$ mm. A uniform sand layer 1 cm thick is spread on the windward side of the barrier between the end-plates. The prototype is tested for six sand levels in order to estimate the evolution of the efficiency of the barrier with increasing sand accumulation. In particular, each initial sand level is set with a 15° degrees slope. From the adopted scaling law follows Reynolds number $\mathrm{Re} = Uh/\nu = 1.8e + 5$, and Froude number for particles saltating in the wind tunnel test section $\mathrm{Fr} = U^2/gH = 4.1$. Re value is within the supercritical aerodynamic regime, where significant Re effects do not take place. Fr value fulfills the limit criterion set by Owen and Gilette [42, 43], being lower than 20.

For each sand level, both the time-evolution of the profile of the accumulated sand upwind of the prototype and the time-evolution of the outgoing sand transport rate above the S4S deflector are measured. A pulsating laser sheet highlights the sand accumulation profile evolution and the saltating sand grains around S4S. The central transparent section allows the acquisition of the profile of the accumulated sand

in the wind tunnel centerline by charged-coupled device imaging of the pulsed-laser sheet scattered from the accumulated sand. Three cameras are installed. Camera #1 captured the whole sand level evolution. Camera #2 and camera #3 captured the saltating particles below and above the barrier deflector, respectively. The same pulsed-laser sheet images are employed to obtain the concentration field of the saltating sand grains *via* the so-called Particle Tracking Velocimetry (PTV) algorithms. The incoming sand transport on a flat surface is measured with the same technique over a uniform sand layer. The incoming wind speed is measured by Particle Image Velocimetry (PIV) technique. The measurement is performed by means of the same laser and cameras using a smoke generator to seed the wind flow with oil particles (Fig. **8**).

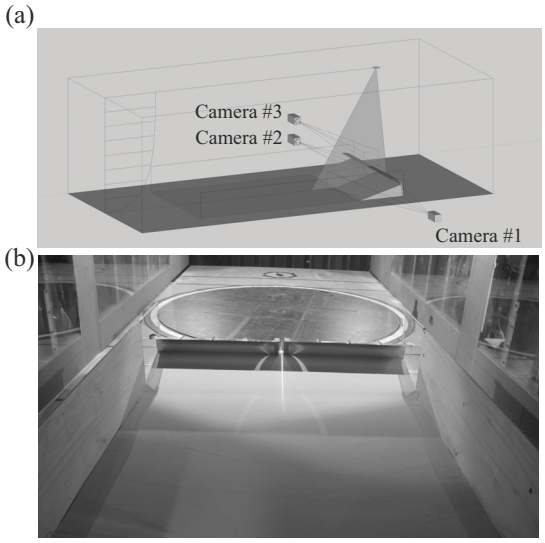

Fig. (8). Wind tunnel setup. Sketch of the setup (a) and testing section (b).

4. RESULTS AND DISCUSSION

First, the results of the aerodynamic comparative analysis between S4S and SVW are presented. Hence, the efficiency of S4S is obtained from the wind tunnel tests.

4.1. Computational Simulation

Computational simulations enable the efficient comparative analysis of the aerodynamic performances of a number of SMMs. For the sake of conciseness, the preliminary estimation of sand trapping performance of S4S barrier is compared with the one resulting from the Straight Vertical Wall (SVW), taken as a reference case. Interested readers can refer to Bruno *et al*. [17] for a wider comparative analysis of the sand trapping performance among a number of other patented solid barriers, *e.g.* [27,28,29]. The barriers have the same height $h = 4\,m$, and are placed at the same distance from the embankment (see Fig. **(7)**), in order to evaluate the performance in the same working conditions.

The computational simulation of the wind flow allows computing wall shear stress on the ground and on the barrier surface. The horizontal and the vertical characteristic sedimentation lengths L_{sx} and L_{sz} can be defined and evaluated in turn (Fig. **9**). The former is the distance between the barrier frontal toe and the point on the ground surface upwind the barrier at which τ becomes smaller or equal to τ_t. The latter is the height of stagnation point on the frontal surface of the barrier. Hence, we define the sand accumulation potential as $A_s \propto L_{sx}L_{sz}$. This quantity can be used to compare the performance of different sand-mitigation barriers, at least in a concept design phase.

As shown in Fig. **(9)**, the barrier induces the formation of an upwind vortex A_r, and a long recirculating wake. Clearly, only the upwind vortex affects sand accumulation on the windward side of the barrier by inducing the sedimentation of the saltating sand particles.

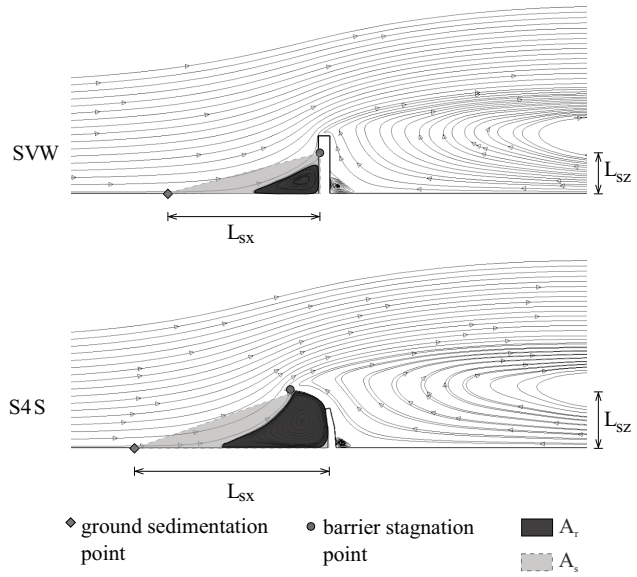

Fig. (9). S4S versus SVW: streamlines around barriers and sedimentation lengths.

The influence of the barrier profile on the flow field is relevant in the upwind zone. The deflector of the S4S barrier leads to twofold effect. First, it drives the stagnation point up to its free end, so that L_{sz} is maximized. Secondly, it induces a horizontal sedimentation length L_{sx} longer than the reference case (SVW), due to the larger size of the upwind recirculation vortex. Altogether, these effects lead to about 100% increment of sand accumulation potential A_s for S4S barrier with respect to SVW, as shown by Fig. (**10**). It is worth stressing that A_s gives only a first estimation of the real sand trapping performance of the analyzed barriers. Indeed, the evaluation of the barrier's efficiency should take into account both barrier aerodynamics, sand transport and sand-bed morphodynamics. The barrier aerodynamics directly affect sand transport, sedimentation and erosion. In turn, the accumulated sand affects the whole aerodynamics. Moreover, close to the ground, the volume fraction of sand is maximum and the dispersed grains tangibly influence wind velocity field. As a result, the sand trapping performance will not be constant.

4.2. Wind Tunnel Testing

In the wake of the extensive computational simulations, wind tunnel tests are limited to the S4S barrier because of their cost and duration. Photos of the sand accumulation levels highlighted by the laser sheet are reported in Fig. **(11)**,

while they are plotted for each sand level at initial (t_0) and final (t_{end}) conditions in Fig. (**12**).

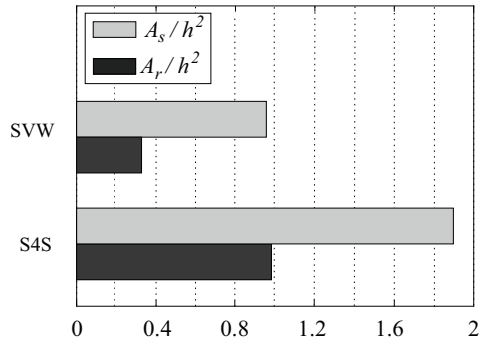

Fig. (10). S4S versus SVW: accumulation potentials and sizes of the upwind vortices.

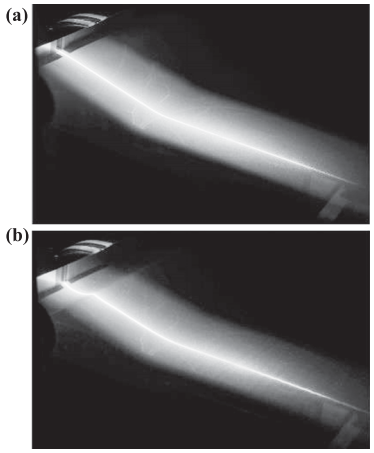

Fig. (11). Sand accumulation profile before (a) and after (b) a generic wind tunnel test.

The sand levels reflect the morphodynamics that takes place upwind the barrier. These results qualitatively confirm the working principles of S4S. In particular, the upwind recirculation vortex induced by S4S promotes reversed sand erosion near the barrier, while the lowering of the wind speed promotes sand sedimentation upwind the eroded zones. The intersection between initial and final sand levels splits erosion and sedimentation zones. Even if the erosion zone gets necessarily shorter as the sand level increases, sedimentation remarkably still holds also for the highest sand level (sand level 5 in Fig. **12**). Moreover, Fig. (**13**) shows both the incoming and outgoing mean sand concentrations φ for each sand accumulation level. They are plotted preserving the same scale in order to have a not misleading graphic representation of the amount of incoming and outgoing sand. The mean incoming sand concentration φ follows a typical decreasing exponential trend and is constant for each sand level. The height of the saltation layer is determined as the height below which 99% of the total concentration take place and is equal to $\delta = 14.4$ cm. The mean outgoing sand concentration profile changes slightly as a function of the filling height.

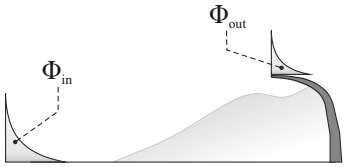

Fig. (13). Efficiency scheme.

The efficiency η of S4S prototype is obtained through the following relation:

$$\eta = \frac{\Phi_{in} - \Phi_{out}}{\Phi_{in}} \quad (5)$$

where Φ_{in} is the integral of the mean incoming sand concentration (Fig. (**13**)) and Φ_{out} is the integral of the mean outgoing sand concentration, both evaluated as

$$\Phi = \int_0^{+\infty} \varphi(z)\ dz. \quad (6)$$

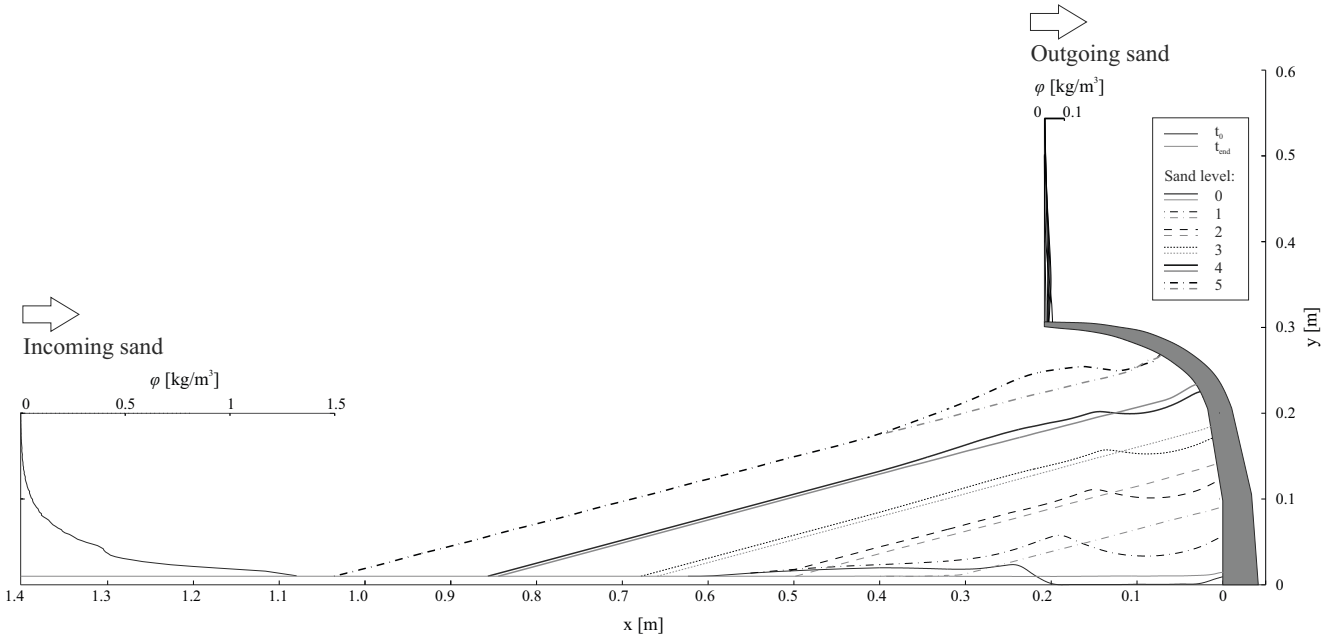

Fig. (12). Sand accumulation profiles against S4S barrier and incoming and outgoing sand concentration $\boldsymbol{\varphi}$.

In Fig. **(14)**, the efficiency assessed from the wind tunnel measurements is plotted as a function of the filling height ratio h_s/h, where h_s is the height of the intersection between the final sand accumulation level (t_{end}) and the barrier profile and h is the height of S4S prototype. The measured efficiency is approximately constant and about 90% for each tested sand level. The dotted curve represents the fitted efficiency trend of S4S. In particular, it is roughly constant for $0 < h_s/h < 0.9$, decreases steeply in order to have a null efficiency for the maximum level of sand accumulation, *i.e.* $h_s = h$. In summary, wind tunnel tests demonstrate S4S traps more than 90% of the incoming sand, and that keeps such high performances up to its maximum capacity. These qualities imply a very small fraction of sand reaches the downwind strip, and permit low frequency sand removal operations, respectively.

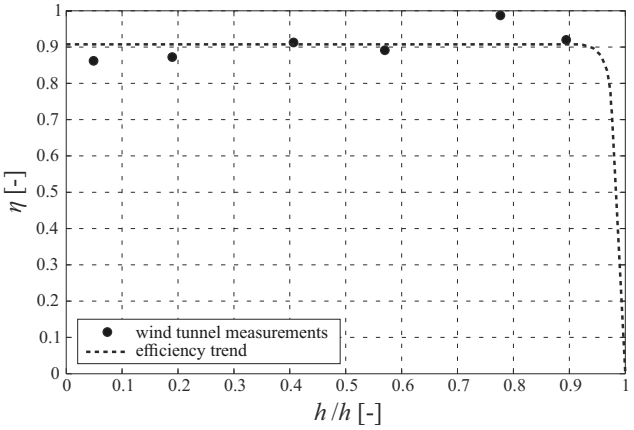

Fig. (14). Efficiency of the S4S prototype.

4.3. S4S Costs and Benefits

The evaluation of the S4S barrier efficiency grounds the estimate of its benefits in term of sand maintenance frequency and cost savings.

In the following, we compare S4S-mitigated railway to an unmitigated one. The incoming sand drift is set equal to 30 m^3/m yr, a typical value in windy desert environments [44]. We adopt a generic double track railway with a 2.5 m high embankment. The S4S height is set equal to 4 m. The downwind strip width is set equal to 10 m. The S4S efficiency refers to the wind tunnel test measurements, while the sedimentation rate upwind the embankment is estimated from the experimental results in Hotta and Horikawa [16].

Sand maintenance is limited to accumulated sand removal and disposal from upwind and downwind strips, and sand fouled ballast cleaning. For the sake of generality, railway Loss of Capacity (LoC) induced by sand maintenance operation is not accounted, because LoC strongly depends on the specific features of each particular railway line. In particular, three distinct maintenance criteria are set depending on the area interested in sand sedimentation (Fig. **2**): i. upwind strip sand removal is planned when S4S efficiency drops under 90%; ii. downwind sand removal is planned when the mean height of sedimented sand passes 25 cm or when the sedimentation rate upwind the embankment drops under 20% in the case of the mitigated and unmitigated railway, respectively; iii. infrastructure ballast cleaning is planned when the percentage void contamination reaches 30% (as stated by Indraratna *et al.* [45]).

For the setup above, the following maintenance periods result (Table **1**):

Table 1. Maintenance Periods.

Maintenance period	*S4S*	*Unmitigated*
Sand removal upwind S4S	2.2 years	-
Sand removal upwind embankment	1.9 years	1 month
Ballast cleaning	3.2 years	10 days

The maintenance frequency around the unmitigated railway is very high. In particular, the ballast cleaning operations are expected to induce severe LoC even for low rail traffic volume. Conversely, S4S dramatically reduces the maintenance frequency, so that maintenance period arises from the order of magnitude of weeks to one of the years. On the basis of the obtained maintenance periods a Life-Cycle Cost Analysis (LCCA, [46]) is carried out, along with the whole service life of the infrastructure set equal to 100 yr. The analysis is limited to the following estimated costs: i. S4S design and construction cost, 1800 \$/m; ii. upwind strip sand removal and disposal cost, 6.9 \$/m^3; iii. downwind sand removal and disposal cost, 7.6 \$/m^3; iv. ballast cleaning cost, 42 \$/m for each track. The railway construction time is set equal to 6 years, and the applied discount rate is 5%. Fig. (**15a**) shows cumulated costs for both unmitigated and S4S-mitigated railway per kilometer. The cumulated savings resulting from the adoption of S4S are reported in Fig. (**15b**). Even if S4S involves initial construction costs, the parity with the costs in the unmitigated scenario takes place after just 1 year after barrier completion, the cost saving obtained with S4S is equal to 20 M\$/km after 20 years, and the final one amounts to over 40 M\$/km.

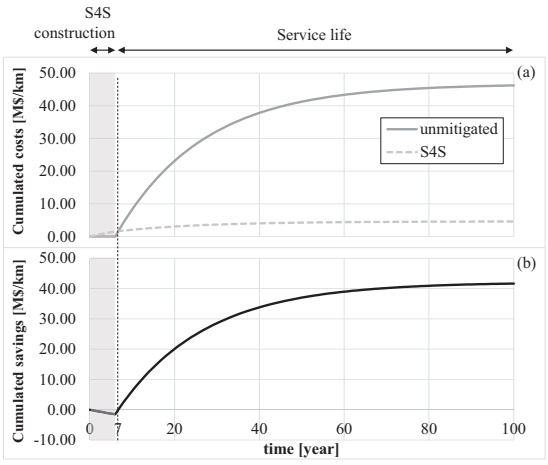

Fig. (15). Life-cycle coast analysis: S4S versus unmitigated railway.

CONCLUSION

Among windblown sand mitigation measures, solid barriers provide some substantial advantages with respect to porous barriers. They manage to trap windblown sand on the upwind strip only and are much more durable with respect to sand fences. The present study shows a novel patented windblown sand solid barrier called Shield for Sand. The so-called sand accumulation potential of S4S is estimated by means of a computational fluid dynamics approach and it is compared with the one of a straight vertical wall. The obtained results clarify S4S working principles and clearly show the performance increment reached in terms of accumulation potential with respect to the straight vertical wall. A wind tunnel test is performed on a prototype of S4S in order to assess its sand trapping efficiency. The results are quite promising since the experimental outcomes confirm the working principle of S4S and its efficiency remains almost constant with increasing sand accumulation.

CURRENT & FUTURE DEVELOPMENTS

Computational simulations and wind tunnel tests have been carried out to validate/demonstrate the performances of the patented technology. They adopt controlled wind and sand conditions commonly encountered in desert environments. In order to obtain the full performance assessment of S4S, we are currently planning full-scale field tests aiming at i. comparing wind tunnel and field measurements and estimating scaling effects, if any; ii. assessing the efficiency under the operational environmental conditions for a given construction site; iii. increasing the TRL of S4S up to TRL8 (as-built design phase).

Future developments include the optimization of the S4S barrier. The S4S barrier is susceptible to be employed along dozen km long railway segments. Hence, optimization can lead to significant costs savings. We are planning aerodynamic shape optimization by means of rigorous computational-based optimization algorithms. The computational simulations will be based on the multiphase wind+sand model we are currently developing [37]. A further optimization is needed to minimize costs and duration of the barrier construction and its maintenance. The optimal construction methods, embodiments and materials for each part of S4S should be selected having in mind the industrial production chain and specific Country where the barrier put in place.

Once optimal S4S setup is defined, a complete life cycle cost analysis will be carried out to quantify the costs and benefits of S4S, compared to other kinds of SMMs.

CONSENT FOR PUBLICATION

Not applicable.

CONFLICT OF INTEREST

The authors declare no conflict of interest, financial or otherwise.

ACKNOWLEDGEMENTS

The study has been developed in the framework of the Windblown Sand Modeling and Mitigation joint research, development and consulting group established between Politecnico di Torino and Optiflow Company (www.polito.it/wsmm). The authors thank the other members of the group for the fruitful discussions about the topic of the paper.

Computational resources were provided by HPC@POLITO, a project of Academic Computing within the Department of Control and Computer Engineering at Politecnico di Torino (http://www.hpc.polito.it).

The S4S patent is owned by Politecnico di Torino and managed by its Technology Transfer and Industrial Liaison Department.

Wind tunnel tests have been accomplished within the "Proof of Concept" programme of Politecnico di Torino, funded by Compagnia di San Paolo.

The Authors wish to thank Jeroen van Beek and Gertjan Glabeke, von Karman Institute for Fluid Dynamics, for their involvement in wind tunnel tests.

REFERENCES

[1] Z. Dong, G. Chen, X. He, Z. Han, and X. Wang, "Controlling blown sand along the highway crossing the Taklimakan Desert", *J. Arid Environ*., vol. 57, pp. 329-344, 2004.

[2] K. C. Zhang, J. J. Qu, K. T. Liao, Q. H. Niu, and Q. J. Han, "Damage by wind-blown sand and its control along Qinghai-Tibet railway in China", *Aeolian Res*., vol. 1, pp. 143-146, 2010.

[3] A. A. Alghamdi, and N. S. Al-Kahtani, "Sand control measures and sand drift fences", *J. Perform. Constr. Facil*., vol. 19, pp. 295-299 2005.

[4] X. M. Wang, C. X. Zhang, E. Hasi, and Z.B. Dong, "Has the three norths forest shelterbelt program solved the desertification and dust storm problems in arid and semiarid China?", *J. Arid Environ*., vol. 74, pp. 13-22, 2010.

[5] K. K. Bofah, and K. G. Al-Hinai, "Field tests of porous fences in the regime of sand-laden wind", *J. Wind Eng. Ind. Aerodyn*., vol. 23, pp. 309-319, 1986.

[6] MEED Insight, "Middle East Rail and Metro Projects Report 2014", 2014.

[7] Executive Intelligence Review, "Iran at the Crossroads of The Eurasian Land-Bridge", 2017.

[8] G. Al-Gassim, "North South railway challenges", Saudi Railway Company, Project Report, Saudi Arabia, 2013.

[9] J. J. Cheng, F. Q. Jiang, C. X. Xue, G. W. Xin, K. C. Li and Y. H. Yang, "Characteristics of the disastrous wind-sand environment along railways in the Gobi area of Xinjiang, China", *Atmos. Environ*., vol. 102, pp. 344-354, 2015.

[10] J. A. Zakeri, M. Esmaeili, S. A. Mosavebi, and R. Abbasi, "Effects of vibration in desert area caused by moving trains", *J. Modern Transport*., vol. 20, pp. 16-23, 2012.

[11] M. Faccoli, C. Petrogalli, M. Lancini, A. Ghidini, and A. Mazzù, "Effect of desert sand on wear and rolling contact fatigue behaviour of various railway wheel steels", *Wear*, vol. 396-397, pp. 146-161, 2018.

[12] J. A. Zakeri, "Investigation on railway track maintenance in sandy-dry areas", *Struct. Infrastruct. Eng.: Maint. Manag. Life-Cycle Des. Perform.*, vol. 8, pp. 135-140, 2012.

[13] B. Li, and D. J. Sherman, "Aerodynamics and morphodynamics of sand fences: A review", *Aeolian Res*., vol. 17, pp. 33-48, 2015.

[14] J. J. Cheng, G. W. Xin, L. Y. Zhi, and F. Q. Jiang, "Unloading characteristics of sand drift in wind-shallow areas along railway and the effect of sand removal by force of wind", *Sci. Rep*., vol. 7, pp. 41462, 2017.

[15] J. Cheng, and C. Xue, "The sand-damage–prevention engineering system for the railway in the desert region of the Qinghai-Tibet plateau", *J. Wind Eng. Ind. Aerodyn*., vol. 125, pp. 30-37, 2014.

[16] S. Hotta, and K. Horikawa, " Function of sand fence placed in front of embankment", In *22nd International Conference on Coastal En-*

gineering, American Society of Civil Engineers, New York, USA, 1991, pp. 2754-2767.

[17] L. Bruno, D. Fransos, and A. Lo Giudice, "Solid barriers for wind-blown sand mitigation: aerodynamic behavior and conceptual design guidelines", *J. Wind Eng. Ind. Aerodyn*., vol. 173, pp. 79-90, 2018.

[18] A. A. A. Alghamdi, and N. S. Al-Kahtani, "Sand control measures and sand drift fences", *J. Perform. Constr. Facil*., vol. 19, pp. 295-299, 2005.

[19] ITALFERR, "Preliminary design for Oman National Railway Project – segment 1 – Oman/UAE border at Al Buraimi - geotechnical study", Sand mitigation report, 2014.

[20] R. Mendez, "La arena invade tramos del ave a la meca ante la divisin del consorcio espaol", El confidencial, 2016.

[21] D. C. Fresno, J. J. Del Coz Dìaz, J. R. Hernàndez, and L. A. S. Fontaneda, "*Barrier for deposition of particles*", WO Patent 2010133713, 2010.

[22] Y. Tang, J. Qu, Z. Ying, F. Zhou, C. Tie, L. Gu, C. Li, W. Rong, and Q. Li, "*High and vertical HDPE (high-density polyethylene) sand-blocking fence*", CN Patent 201686941, 2010.

[23] J. J. Grosch, and N. S. Kahtani, "*Geogrid sand fence*", WO Patent 201059597, 2010.

[24] F. Jiang, K. Li, C. Xue, L. Ding, L. Zhang, Y. Yang, and Y. Da, "*Wind and sand shielding device*", CN Patent 201817781 U, 2010.

[25] C. Li, H. Dong, Y. Shi, Z. Jun, H. Li, and X. Wang, "*Sandproof railing of hung concrete upper block board*", CN patent 200996134 U, 2007.

[26] X. Fang, L. Xiao, X. Wang, H. Yao, Y. Ma, F. Li, and H. Jia, "*Novel wind break fence is moduled to wood*" CN Patent 205063528 U, 2016.

[27] J. P. Newell, "*Sand guards for railroad tracks*". U.S. Patent 731320, 1903.

[28] M. Pensa, P. S. Petrosino, and G. S. Petrosino "*Barriera antivento, particolarmente per venti carichi di sabbia*" IT Patent 1224625, 1990.

[29] L. Guangyong, and M. Peng, "*Wind-preventing sand-throwing wall*" CN Patent 102002916 B, 2011.

[30] N. Takashi, "*Protection fence*" JP Patent 3138408, 2007.

[31] A. Sato, and M. Ono, "*Snowstorm guard fence structures and jet roofs*", U.S. Patent 4958806, 1990

[32] L. Wei, "*Flow-diverting and wind-curbing road-protection wall for desert highway*" CN Patent 101761037 B, 2010.

[33] L. Bruno, L. Preziosi, and D. Fransos, "*A defecting module for an anti-sand barrier, a barrier thus obtained and a protection method from windblown sand*" WO Patent 2016181417, 2016.

[34] A. Schmidt, Santera 3000 technical sheet, 2013.

[35] L. Raffaele, L. Bruno, F. Pellerey, and L. Preziosi, "Windblown sand saltation: A statistical approach to fluid threshold shear velocity", *Aeol. Res*., vol. 23, pp. 79-91, 2016.

[36] S. R. Sadin, F. P. Povinelli,, and R. Rosen, "The NASA technology push towards future space mission systems," *Acta Astronautica*, vol. 20, pp. 73-77, 1989.

[37] L. Preziosi, L. Bruno, and D. Fransos, "A multiphase first order model for non-equilibrium sand erosion, transport and sedimentation", *Appl. Math. Lett*., vol. 45, pp. 69-75, 2015.

[38] L. Bruno, A. Lo Giudice, L. Preziosi, and L. Raffaele, "Wind tunnel tests of the shield for sand barrier", Final Internal Technical Report, Proof of Concept programme, Politecnico di Torino, 2017.

[39] F. R. Menter, "Two-equation eddy-viscosity turbulence models for engineering applications", *AIAA J.*, vol. 32, pp. 1598-1605, 1994.

[40] F. R. Menter, M. Kuntz, and M. R. Langtry, "Ten years of industrial experience with the SST turbulence model", In *Proceedings of the Fourth International Symposium on Turbulence, Heat and Mass Transfer*, Antalya, Turkey, 2003, 625-632.

[41] P. Richard, and S. Norris, "Appropriate boundary conditions for computational wind engineering models revisited", *J. Wind Eng. Ind. Aerodyn.*, vol. 99, pp. 257-266, 2011.

[42] P. R. Owen, and D. Gillette, "Wind tunnel constraint on saltation*". Proc. International Workshop on the Physics of Blown Sand*, University of Aarhus, Denmark, 1985, pp. 253-269.

[43] B. R. White, and H. Mounla, "An experimental study of Froude number effect on wind-tunnel saltation", *Acta Mechanica*, vol. 1, pp. 145-157, 1991.

[44] L. Raffaele, L. Bruno, F. Pellerey, and D. Fransos, "Incoming windblown sand drift to civil infrastructures: A probabilistic evaluation", *J. Wind Eng. Ind. Aerodyn*, vol. 166, pp. 37-47, 2017.

[45] B. Indraratna, L. Su, and C. Rujikiatkamjorn, "A new parameter for classification and evaluation of railway ballast fouling", *Can. Geotech. J.*, vol. 48, pp. 322-326, 2011.

[46] W. Fabrycky, and B. Blanchard, "Life cycle cost and economic analysis". New Jersey: Prentice Hall, 1991.